

Thermal monopoles and selfdual dyons in the Quark-Gluon Plasma

M.N. Chernodub,^{1,2,3} A. D’Alessandro,⁴ M. D’Elia,⁴ and V.I. Zakharov^{3,5}

¹ CNRS, LMPT, Fédération Denis Poisson, Université de Tours, F-37200, Tours, France

² DMPA, University of Gent, Krijgslaan 281, S9, B-9000 Gent, Belgium

³ ITEP, B. Chermushkinskaya 25, Moscow, 117218, Russia

⁴ Dipartimento di Fisica, Università di Genova and INFN, Via Dodecaneso 33, I-16146 Genova, Italy

⁵ Max-Planck-Institut für Physik, Föhringer Ring 6, 80805 München, Germany

(Dated: September 26, 2009)

We perform a numerical study of the excess of non-abelian gauge invariant gluonic action around thermal abelian monopoles which populate the deconfined phase of Yang-Mills theories. Our results show that the excess of magnetic action is close to that of the electric one, so that thermal abelian monopoles may be associated with physical objects carrying both electric and magnetic charge, i.e. dyons. Thus, the quark gluon plasma is likely to be populated by selfdual dyons, which may manifest themselves in the heavy-ion collisions via the chiral magnetic effect. Thermodynamically, thermal monopoles provide a negative contribution to the pressure of the system.

PACS numbers: 12.38.Aw, 25.75.Nq, 11.15.Tk

I. INTRODUCTION

Interpretation of heavy ion experiments at RHIC and first-principle lattice simulations suggest that the quark-gluon plasma has quite unusual properties [1]. Contrary to general expectations, at temperatures just above the critical temperature, T_c , the plasma looks like an ideal fluid rather than a system of weakly interacting quark-gluon gas. The reason of this behavior lies in the strongly interacting nature of the quark-gluon plasma.

The magnetic component of the gluon fields may be a key player in the unusual dynamics of the plasma [2, 3, 4, 5, 6, 7, 8, 9]. The basic idea underlying the magnetic picture can be motivated in the following way [2]. As it was suggested long time ago in Ref. [10], at low temperatures the magnetic degrees of freedom exist in the form of a (gluo)magnetic condensate. Magnetic charge condensation is believed to be responsible for color confinement and this is usually known as the dual superconductor scenario: the existence of such condensation and its disappearance at the critical temperature T_c has been verified in various lattice QCD studies (see e.g. Refs. [11, 12, 13, 14] or Ref. [15] for a review). As the temperature increases, the condensate starts to evaporate and it is destroyed completely at T_c , while the magnetic color degrees are released as thermal states into the gluon plasma. The central point is that simultaneously the magnetic degrees of freedom are to become physical and constitute a real, thermally excited component of the gluon plasma [2].

The magnetic monopoles in the Yang-Mills plasma are particlelike objects made of gluons. The monopoles are suggested to affect both the transport properties and the thermodynamical features of the plasma [2, 3, 9]. This suggestion can in principle be checked by numerical simulations of Yang-Mills theory on the lattice. The lattice method provides us with thermalized ensembles of monopole trajectories in Euclidean space time. However, in order to calculate the contribution of thermal (i.e.,

real) monopoles to any physical quantity one should be able to separate the thermal monopoles from numerous virtual monopole loops. Virtual monopoles – which are responsible essentially for ultraviolet physics – are known to populate the thermal ensembles in numerous quantities, so that the separation of monopoles into real and virtual parts seems to be a difficult task.

It was shown in Ref. [2] that thermal monopoles in Minkowski space-time are associated with Euclidean monopole trajectories that have a nontrivial wrapping number on the short (thermal) direction of the Euclidean space. Moreover, the density of the monopoles in the Minkowski space-time is given by the thermal average of the absolute value of the monopole wrapping number. The properties of the wrapped trajectories were studied numerically using lattice simulations in Ref. [4, 16]. In Ref. [4] the average wrapping number of the monopole trajectories was thoroughly calculated. It was shown that this quantity is free from ultraviolet artifacts as it should be the case for a purely thermal quantity. The monopole density grows with the temperature T . However, the parametrical T -dependence of this quantity differs from the behavior expected in the case of an ideal gas of the monopoles. This is one of the first lattice evidences on the nontrivial dynamics of the magnetic monopoles in the high temperature gauge theory [4].

Monopoles do not appear alone in the plasma. Numerical simulations have revealed the fact that monopoles are a part of chainlike structures [15]. In these structures the (anti)monopoles are connected to each other by magnetic vortices. The existence of the vortex defects is related to the nontriviality of the center of the gauge group. Both the monopoles and vortices contribute to the equation of state of Yang-Mills theory at finite temperature [5, 6] (a short review of the subject can be found in Ref. [8]).

A calculation of the effect of the vortices on the pressure of the Yang-Mills plasma can be formulated in a rather straightforward and clear way. According to Ref. [5] the vortices provide a negative contribution to

the pressure in agreement with theoretical expectations of Ref. [7]. As for the monopoles, the preliminary calculation of Ref. [6] indicated that they provide a large positive contribution. However, the calculation was done using a nonlocal method which did not discriminate between the real and virtual monopole loops. Below we show that the contribution of the *thermal* monopoles to the pressure of gluons is negative as well.

Thermal monopoles detected by lattice QCD simulations are of abelian nature. An abelian projection is needed to define magnetic monopole currents (see the Appendix for details) and the Maximal Abelian Gauge (MAG) is usually chosen to do that. The fact that both the density and the spatial correlations of thermal monopoles measured in the MAG projection are free of UV artifacts [4] (i.e. they correctly scale to the continuum limit) points to an underlying physical meaning of those objects. Nevertheless, the dependence on the chosen abelian projection still poses a problem. In order to further investigate this issue and better clarify the physical properties of thermal monopoles, we have decided to measure the correlation of the unprojected gauge invariant nonabelian action density with the positions of abelian thermal monopoles. As we shall clarify in the following, this is also the essential quantity entering the determination of thermodynamic properties of thermal monopoles (e.g. their contribution to the pressure).

We made refined measurements which treat the magnetic and electric parts of the gluon action separately. This allowed us to find – as an unexpected byproduct – that the excesses of the magnetic and electric action densities have almost the same value near the monopoles suggesting that the electric and magnetic components of these objects have the same significance. We conclude that the objects which we identified simply as thermal abelian monopoles after abelian projection, may correspond to more interesting physical objects, actually thermal dyons, with equal electric and magnetic charges [17]

The dyons in zero-temperature Euclidean Yang-Mills theory were discussed in the literature for a long time both in continuum [18] and lattice [19, 20] formulations. In Ref. [20] smooth dyonic solutions were observed in the deconfinement phase of lattice Yang-Mills theory. Here we discuss another lattice evidence in favor of existence of dyons as real objects in quark gluon plasma. It is necessary to mention that these dyons would have a finite density which is independent of the ultraviolet cutoff.

The importance of non-Abelian dyons in the quark gluon plasma is difficult to overestimate since these objects may play a key role in the so-called chiral magnetic effect. This effect – which reveals certain CP -odd correlations in the quark-gluon plasma – was suggested theoretically in Ref. [21]. The chiral magnetic effect leads to generation of an electric current along the direction of a magnetic field in a nontrivial topological backgrounds of gluons. The strong magnetic field is naturally created in heavy-ion collisions, and the appearance of the electric current is detected in a form of a certain geometric

asymmetry of electrically charged particles produced in the collisions. There are preliminary indications that the chiral magnetic effect has been indeed observed by the STAR Collaboration in experiments at RHIC [22]. The signatures of this phenomenon were also found in recent numerical lattice simulations [23], and discussed in non-perturbative holographic approaches of Ref. [24]. In case the dyons are really associated to the thermal monopoles, as suggested by our results, they may serve as fluctuations of the topological charge in the quark gluon plasma phase.

The structure of this paper is as follows. In Sec. II we review basic thermodynamical relations of Yang-Mills theory. In Sec. III we formulate how to estimate the influence of the monopoles on thermodynamics and how to calculate the electric and magnetic action densities around the monopoles. In Sec. IV we present our numerical results. Our conclusion is summarized in the last Section, and technical details are given in the Appendix.

II. THERMODYNAMICS OF GLUONS

The partition function of the Yang–Mills theory is

$$\mathcal{Z} = \int \text{DA} \exp \left\{ -\frac{1}{2g^2} \text{Tr} G_{\mu\nu}^2 \right\}, \quad (1)$$

where $G_{\mu\nu} = G_{\mu\nu}^a t^a$ is the field strength tensor of the non-Abelian field A , and t^a are the $SU(N)$ generators normalized in the standard way, $\text{Tr} t^a t^b = \frac{1}{2} \delta^{ab}$.

For a sufficiently large and homogeneous gluon system residing in thermodynamical equilibrium the pressure p and the energy density ε are given by the derivatives of the partition function (1) with respect to the spatial volume, V , and the temperature T , respectively,

$$p = \frac{T}{V} \frac{\partial \log Z(T, V)}{\partial \log V} = \frac{T}{V} \log Z(T, V), \quad (2)$$

$$\varepsilon = \frac{T}{V} \frac{\partial \log Z(T, V)}{\partial \log T}, \quad (3)$$

Following a standard approach (see, e.g., Ref. [25]), one can relate the energy density ε and the pressure p can via the quantum average the trace of the energy–momentum tensor $T_{\mu\nu}$,

$$\theta(T) = \langle T_{\mu}^{\mu} \rangle \equiv \varepsilon - 3p, \quad (4)$$

where in Yang–Mills theory

$$T_{\mu\nu} = 2 \text{Tr} \left[G_{\mu\sigma} G_{\nu\sigma} - \frac{1}{4} \delta_{\mu\nu} G_{\sigma\rho} G_{\sigma\rho} \right]. \quad (5)$$

At the classical level trace of this quantity is zero because the *bare* Yang–Mills theory is a conformal theory. However, at the quantum level the conformal invariance is broken, and, consequently, the energy–momentum tensor exhibits a trace anomaly: the quantum average of the

trace of the energy momentum tensor (4) is nonzero. The trace anomaly is intimately related to the gluon condensate which breaks the scale invariance of the theory

$$\theta(T) = \left\langle \frac{\tilde{\beta}(g)}{2g} G_{\mu\nu}^a G_{\mu\nu}^a \right\rangle, \quad (6)$$

where $\tilde{\beta}(g)$ the Gell-Mann-Low β -function. We use the notation $\tilde{\beta}$ instead of the conventional β in order to avoid a confusion with the lattice coupling constant

$$\beta = \frac{2N}{g^2}. \quad (7)$$

The trace anomaly (4) is an important thermodynamic quantity because it allows us to reconstruct both the pressure and the energy density as follows:

$$p(T) = T^4 \int_0^T \frac{dT_1}{T_1} \frac{\theta(T_1)}{T_1^4}, \quad (8)$$

$$\varepsilon(T) = 3T^4 \int_0^T \frac{dT_1}{T_1} \frac{\theta(T_1)}{T_1^4} + \theta(T). \quad (9)$$

On the lattice the dynamical fields are the gluonic $SU(N)$ matrices $U_{x\mu}$ which are identified at the lattice links $l = \{x, \mu\}$. The link gauge fields are related to the continuum gauge fields $A_\mu(a)$ in the limit of vanishing lattice spacing, $a \rightarrow 0$:

$$\begin{aligned} U_{x\mu} &= \exp \left\{ ig \int_x^{x+a\hat{\mu}} dy A_\mu(y) \right\} \\ &\rightarrow \mathbb{1} + iagA_\mu(x) + O(a^2), \end{aligned} \quad (10)$$

The lattice spacing a is a function of the lattice coupling (7).

The lattice analogue of the partition function (1) is

$$\mathcal{Z}(T, V) = \int DU \exp \left\{ -\beta \sum_P S_P[U] \right\}. \quad (11)$$

where the plaquette action density $S_P[U]$ is usually written in the Wilson form,

$$S_P[U] = 1 - \frac{1}{N} \text{Re Tr } U_P, \quad U_P = \prod_{l \in \partial P} U_l, \quad (12)$$

The spatial volume $V = (L_s a)^3$ and the temperature

$$T = \frac{1}{L_t a} \quad (13)$$

of the gluonic system are defined by the asymmetric geometry of the Euclidean lattice, $L_s^3 L_t$. The shorter direction, L_t with $L_t \leq L_s$, is associated with the imaginary time, or, “temperature” direction. The trace anomaly (6) on the lattice is written as follows

$$\frac{\theta(T)}{T^4} = 6 L_t^4 \left(\frac{\partial \beta(a)}{\partial \log a} \right) \cdot \left(\langle S_P \rangle_T - \langle S_P \rangle_0 \right). \quad (14)$$

where $\langle S_P \rangle_T$ and $\langle S_P \rangle_0$ are the action densities at $T > 0$ and at $T = 0$. The subtraction of the $T = 0$ value is needed to remove the effect of quantum fluctuations, which lead to ultraviolet (UV) divergency of the quantum expectation value. The regularized trace anomaly (14) is an UV-finite quantity.

We used the Monte Carlo simulations on the lattice to evaluate the influence of the monopoles on the trace anomaly, and, consequently, on the equation of state in the thermal Yang-Mills theory. We describe setup of our numerical simulations in Appendix A.

III. LOCAL ACTION DENSITIES

The (chromo)magnetic monopoles in the Yang-Mills plasma are particlelike objects made of gluons which are generally believed to be responsible for color confinement in QCD. The monopole confinement scenario is reviewed in Ref. [15]. On the lattice the monopoles appear in the form of the closed trajectories. The monopole loops may be either wrapped around the short (imaginary time) direction of the lattice, or they may form shrinkable loops with zero winding number. The monopole configurations with nontrivial winding are associated with thermal monopoles [2], while the other trajectories correspond to virtual loops. The properties of the winding trajectories were studied long ago in Ref. [26, 27]. A recent study [4] has revealed that the thermal monopole density,

$$\rho = \frac{1}{V_{3D}} \left\langle \sum_{\vec{x}} |N_{\text{wrap}}[m_0(\vec{x}, t)]| \right\rangle, \quad V_{3D} = L_s^3, \quad (15)$$

identified as a density of the average wrapping number [2] $N_{\text{wrap}}[m_0(\vec{x}, t)]$, shows a very good scaling towards a continuum limit. This result confirms the physical nature of thermal, or real, magnetic monopoles in the Yang-Mills plasma.

Expression (6) implies that if the monopoles affect the gluonic condensate then the monopoles should also make influence on the trace anomaly and, as a consequence, on the equation of state of the gluon plasma. Translated to the lattice language (14), this statement means that the thermal monopoles contribute to equation of state if they affect the expectation value of the plaquette action S_P .

At zero temperature the correlation of the monopoles with the action density was indeed established in Refs. [28, 29, 30]. Although this result was obtained in a cold vacuum, it provides us with a hint to suspect that the monopoles may contribute to the equation of state at finite temperature as well.

In the continuum limit, the averaged value of the action density at the position of monopoles can be calculated with the help of the normalized correlator between the monopole trajectory $j_\mu(x)$ and the non-Abelian action density,

$$\langle S \rangle_{\text{mon}}(x, x') \equiv \frac{1}{2g^2} \langle \text{Tr } G_{\mu\nu}^2 \rangle_{\text{mon}}(x, x') \quad (16)$$

$$= \frac{1}{\langle j_\beta^2(x) \rangle} \left\langle j_\alpha^2(x) \frac{1}{2g^2} \text{Tr} G_{\mu\nu}^2(x') \right\rangle.$$

The points x and x' are very close to each other. As we will see below the lattice provides a natural regularization of the correlation function in Eq. (16).

The contribution of the monopoles (16) to the gluon energy density (or, equivalently, to the gluonic condensate) can be subdivided into the electric and magnetic parts, respectively:

$$\langle S \rangle_{\text{mon}} = \langle S_M \rangle_{\text{mon}} + \langle S_E \rangle_{\text{mon}}. \quad (17)$$

The magnetic part of the action density can naturally be expressed as follows [28]:

$$\langle S_M \rangle_{\text{mon}}(x, x') = \frac{1}{\langle j_\alpha^2(x) \rangle} \left\langle \frac{1}{2g^2} \text{Tr} [j_\mu(x) \tilde{G}_{\mu\nu}(x')]^2 \right\rangle \quad (18)$$

where

$$\tilde{G}_{\mu\nu}(x) = \frac{1}{2} \varepsilon_{\mu\nu\alpha\beta} G_{\alpha\beta}(x). \quad (19)$$

If the monopole is static, $j_\mu \sim \delta_{\mu 4}$ then only spacelike (magnetic) components of the field strength tensor G_{ij} with $i, j = 1, 2, 3$ contribute to the correlator (18).

The excess of the chromoelectric action around the monopoles with respect to the chromoelectric vacuum expectation value in the bulk can be evaluated with the help of the following normalized correlator [29]:

$$\langle S_E \rangle_{\text{mon}}(x, x') = \frac{1}{\langle j_\alpha^2(x) \rangle} \left\langle \frac{1}{2} \text{Tr} [j_\mu(x) G_{\mu\nu}(x')]^2 \right\rangle. \quad (20)$$

If the monopole is static, $j_\mu \sim \delta_{\mu 4}$ then only timelike (electric) components of the field strength tensor G_{4i} with $i = 1, 2, 3$ contribute to the correlator (20).

IV. LATTICE RESULTS

A. Lattice observables

The continuum definitions (18) and (20) can be translated to the lattice as follows. First, we locate the wrapped monopole trajectories using a standard prescription described in Appendix A. The monopole current is defined on the links $\{x, \mu\}^*$ of the dual lattice and takes integer values, $j_\mu(x) = 0, \pm 1, \dots$. Usually the multiple-charged currents with $|j_\mu(x)| \geq 2$ are very rare, so that one can set $|j_\mu(x)| = j_\mu^2(x)$ with a high accuracy. Each link $\{x, \mu\}^*$ of the dual lattice corresponds to the 3-cube $\mathcal{C}_\mu(x)$ of the original lattice. Then Eq. (18) in continuum has the following lattice analogue [28]:

$$\langle S_M \rangle_{\text{mon}} = \left\langle \sum_x \sum_{\mu=1}^4 j_\mu^2(x) \right\rangle^{-1} \quad (21)$$

$$\cdot \left\langle \sum_x \sum_{\mu=1}^4 j_\mu^2(x) \left[\frac{1}{6} \sum_{P \in \partial \mathcal{C}_\mu(x)} \left(1 - \frac{1}{2} \text{Tr} U_P \right) \right] \right\rangle,$$

where the sum over plaquettes is taken over all six faces P of the 3-cube $\mathcal{C}_\mu(x)$.

The lattice definition (21) corresponds to a minimal splitting between the points x and x' in the continuum expression (18). The center of the monopole coincides with the center of the 3-cube $\mathcal{C}_\mu(x)$ which surrounds the monopole. On the other hand the monopole contribution (21) to the magnetic part gluon action density is defined by the average of the plaquettes at the faces of the cube. Thus, there is a minimal distance between the monopole position and the point where the gluonic action density is measured. Thus, the lattice formulation (21) of the magnetic correlator (18) provides us with a natural definition of the splitting between the points x and x' . The minimal distance equals to the half lattice spacing a :

$$r_M(a) = \frac{a}{2}. \quad (22)$$

The lattice analogue of the chromoelectric correlator (20) is [28]:

$$\langle S_E \rangle_{\text{mon}} = \left\langle \sum_x \sum_{\mu=1}^4 j_\mu^2(x) \right\rangle^{-1} \quad (23)$$

$$\left\langle \sum_x \sum_{\mu=1}^4 j_\mu^2(x) \left[\frac{1}{24} \sum_{P \in \partial \mathcal{P}[\mathcal{C}_\mu(x)]} \left(1 - \frac{1}{2} \text{Tr} U_P \right) \right] \right\rangle,$$

where one of the sums is taken over 24 plaquettes P which form a manifold $\mathcal{P}[\mathcal{C}_\mu(x)]$ corresponding to the 3-cube $\mathcal{C}_\mu(x)$. This manifold is represented by a set of all plaquettes P which satisfy the following two conditions:

- (i) each plaquette have one, and only one, common link l_ν with the cube $\mathcal{C}_\mu(x)$;
- (ii) each plaquette is lying in the planes, defined by the vectors μ (the direction of the monopole current) and ν (the direction of the link defined in the previous condition).

One can estimate a minimal distance between the gluonic operator S_P and the position of the monopole in the lattice formulation (23) of the electric correlator (20):

$$r_E(a) = \frac{a}{\sqrt{2}}. \quad (24)$$

In order to make this estimation we assumed that the monopole trajectory is static. This assumption is justified because as the temperature increases the zeroth Matsubara component for all bosonic fields – including the monopole trajectories – becomes dominant.

The excess of the magnetic and electric parts of the gluonic action due to the presence of the monopoles is given by the following formulae, respectively,

$$\delta S_A = \langle S_A \rangle_{\text{mon}} - \langle S_A \rangle_{\text{vac}}, \quad A = M, E. \quad (25)$$

where $\langle S_A \rangle_{\text{vac}}$ is the magnetic (for $A = M$) and electric (for $A = E$) action densities in the vacuum:

$$\langle S_M \rangle_{\text{vac}} = \frac{1}{3L_s^3 L_t} \left\langle \sum_{P_{\text{spat}}} \left(1 - \frac{1}{2} \text{Tr} U_{P_{\text{spat}}} \right) \right\rangle, \quad (26)$$

$$\langle S_E \rangle_{\text{vac}} = \frac{1}{3L_s^3 L_t} \left\langle \sum_{P_{\text{temp}}} \left(1 - \frac{1}{2} \text{Tr} U_{P_{\text{temp}}} \right) \right\rangle. \quad (27)$$

Here the sums go over spatial (P_{spat}) and temporal (P_{temp}) plaquettes, respectively.

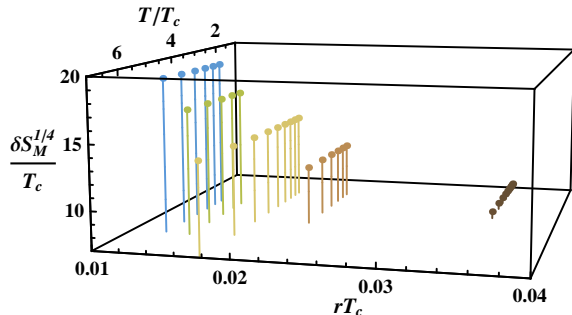


FIG. 1: The excess of the magnetic component δS_M of the gluonic action (25) as the function of the distance r , Eq. (22) from the monopole and the temperature. All quantities are given in units of the critical temperature T_c .

B. Observation of electromagnetic duality

In Fig. 1 we plot the excess of the magnetic component δS_M of the gluonic action (25) over the corresponding vacuum expectation value: results are reported in dimensionless units and as a function of the distance r from the monopole center and of the temperature. We include into this figure all available data sets which are described in Appendix A in more details. Notice that available data refer to a single value of r for each fixed value of the UV cutoff, so that results reported in Fig. 1 have been obtained by collecting together data from different simulations performed at different values of the lattice spacing. Therefore the dependence of δS_M on r , as reported in Fig. 1, cannot be disentangled from a possible dependence of δS_M on the UV cutoff: more simulations in which the non-abelian action density is measured at more than one value of r for each lattice spacing would be necessary to completely address this issue. For that reason, our present discussion about the dependence of δS_M on r should be considered as preliminary and qualitative.

The excess of the magnetic action near thermal monopoles turns out to be a positive quantity at all distances r from the monopole (22) and at all temperatures, moreover it decreases as a function of r . This is an unexpected result because at zero temperature the condensed monopoles have an excess density of magnetic action which, even if still positive, increases as a function of

r , i.e. it is minimum at the monopole center [30]. As the monopoles from the condensate evaporate into the thermal monopoles, one could expect that in the deconfinement phase the excess of the action near monopoles has the same qualitative features as below T_c . This expectation turns out to be not the case, however. The dependence on T is much milder than that on r : the excess of the magnetic action is almost temperature-independent. The same qualitative features are also seen for the electric part of the action, which we show in Fig. 2.

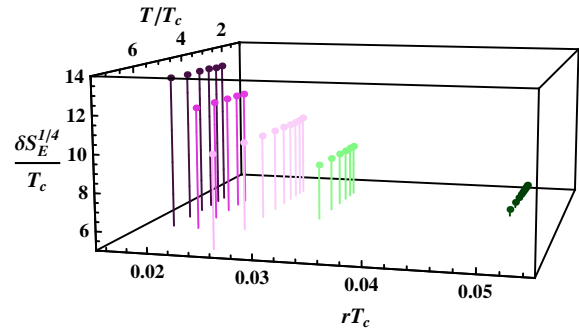


FIG. 2: The same as in Fig. 1 but for the electric part δS_E . The distance is defined by Eq. (24).

It is interesting to note that the electric and magnetic contributions practically coincide with each other,

$$\langle E^2 \rangle \approx \langle B^2 \rangle, \quad (28)$$

where

$$E^2 = \frac{1}{2} G_{0i}^2(x) \quad \text{and} \quad B^2 = \frac{1}{4} G_{ij}^2(x), \quad (29)$$

are the electric and action densities, respectively [in our units Eq. (28) means $\delta S_M \approx \delta S_E$]. On the contrary, for a purely “chromoelectric” object, like quark, one expects

$$\langle E^2 \rangle_{\text{quark}} \neq 0, \quad \text{and} \quad \langle B^2 \rangle_{\text{quark}} \sim 0, \quad (30)$$

while for a purely “chromomagnetic” object, like a monopole, one should get an opposite relation,

$$\langle E^2 \rangle_{\text{mon}} \sim 0, \quad \text{and} \quad \langle B^2 \rangle_{\text{mon}} \neq 0. \quad (31)$$

In Fig. 3 we graphically demonstrate the validity of Eq. (28) by plotting the overlap of the Figs. 1 and 2. For convenience, we show the both contributions to the energy density multiplied by the distance r . Basically, Fig. 3 represents a scaled projection of Figs. 1 and 2 onto the distance-action plane. This figure illustrates the amazing fact that the electric and magnetic actions are the same around the “monopoles”. Indeed, the fact, that the electric and magnetic contributions are almost the same is unusual because from the first principles we would expect that the magnetic component of the gluonic action near the monopole is much stronger than the electric part of the gluonic action.

Even if the equality of electric and magnetic contribution is observed only on average quantities, it is tempting

to make the hypothesis that thermal abelian monopoles are associated to non-abelian field configurations possessing EM duality, i.e. selfdual objects. Numerically, the deviations from the EM duality do not exceed 3.5%.

The objects which carry equal amounts of electric and magnetic components are non-Abelian dyons. The (classical) fields of dyons satisfy the selfduality relation

$$G_{\mu\nu} = \tilde{G}_{\mu\nu}, \quad \tilde{G}_{\mu\nu} = \frac{1}{2}\epsilon_{\mu\nu\alpha\beta}G_{\alpha\beta}, \quad (32)$$

so that electric and magnetic action densities (29) of the dyons are the same,

$$E_{\text{dyon}}^2 = B_{\text{dyon}}^2. \quad (33)$$

This equation is in line with our numerical observation (28).

The simplest selfdual configuration is a (static) Bogomolny–Prasad–Sommerfield (BPS) solution to the classical equations of motion of $SU(2)$ Yang–Mills theory [31]:

$$A_i^a = \frac{1}{g}f(r)\epsilon_{iab}\frac{x^b}{r}, \quad f(r) = \frac{1}{r}\left(1 - \frac{r}{\sinh r}\right), \quad (34)$$

$$A_4^a = \frac{1}{g}h(r)\frac{x^a}{r}, \quad h(r) = \frac{1}{r}(r \coth r - 1). \quad (35)$$

Here the distance coordinates $r \equiv |\vec{x}|$ and x are scaled by an arbitrary factor, $r \rightarrow r_0 \cdot r$, to make a dimensionless quantity.

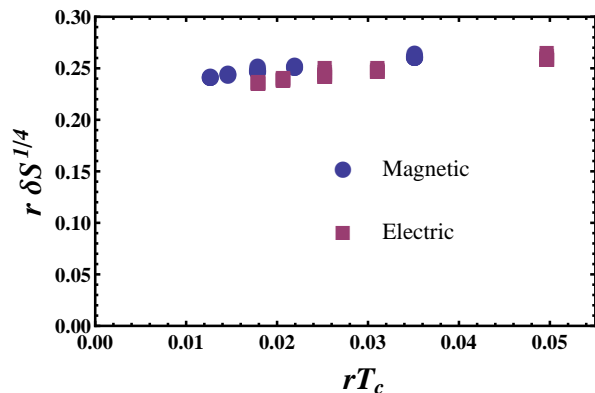


FIG. 3: Illustration of the dyonic nature of the objects: The magnetic (the filled circles) and electric (the filled squares) contributions to (the square root of) the action density multiplied by the distance r as the function of r . The statistical error bars are much smaller than the symbols used.

In order to characterize both the singularity at the origin of the thermal monopole (dyon) and the observed EM duality we fit the magnetic and electric excesses of the action density by the function

$$\delta S_\ell = \left(\frac{C_\ell}{r}\right)^4. \quad (36)$$

We performed three different fits. We fitted the electric action density, $\ell = E$ and, separately, the magnetic

action density, $\ell = M$, and finally, we made the fit of the both simultaneously, $\ell = EM$. In all these fits we have averaged our data points corresponding to different temperatures T and the same distances r (this is a legitimate operation since the data are almost T -independent as one can see from Fig. 3). The best fit parameters are, respectively:

$$\begin{aligned} C_E &= 0.243(2), \\ C_M &= 0.247(2), \\ C_{EM} &= 0.246(2). \end{aligned} \quad (37)$$

These values are very close to each other, so that the duality (28) works with a high precision. In Fig. 4 we plot the joint fit $\ell = EM$ in order to illustrate the quality of the selfduality relation (28). Thus, in this paper we refer to these objects as both monopoles and selfdual dyons simultaneously, because they are identified as monopoles by their magnetic charge, while their non-Abelian content shows signatures of the dyonic selfduality.

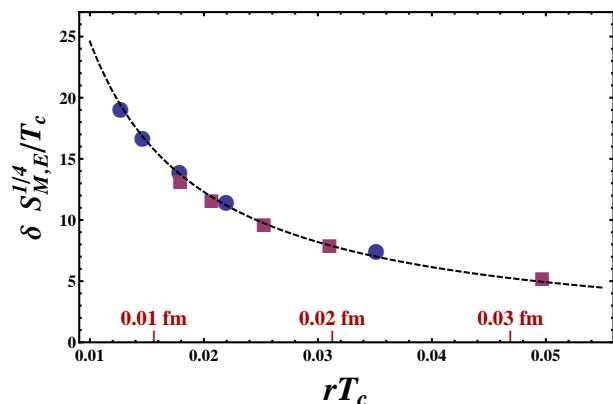


FIG. 4: The fit of the excesses in the magnetic (the blue circles) and electric (the red squares) action densities near the monopole as the function of the distance r from the monopole (shown both in units of T_c^{-1} and in Fermi). The error bars and the magnitude of the temperature dependence is much smaller than the size of the symbols. The data are fitted by the function (36). The fit is shown by the dashed line.

Note that (smooth) dyonic configurations were found in Ref. [20] using a method of cooling of the gluon configurations and/or utilizing the low-lying fermion modes to filter the positions of the dyons. In this paper, assuming that thermal monopoles are indeed associated with dyons, we report the *direct* observation of dyons in dynamical (uncooled) configurations. In fact, the field of the classical BPS dyon (34), (35) is a smooth function at the origin, $r = 0$. On the contrary, our data suggest that the action of the thermal dyons behave as singular as $1/r^4$. One would conclude that quantum thermal dyons are not resembling the smooth classical BPS solutions at all. On the other hand, as already stressed above, our measurements have been taken at the scale of the lattice spacing, so that the dependence on r cannot really be disentangled from that on the UV cutoff and our discussion about the $1/r^4$ behavior should be regarded as

only qualitative: more refined measurements should be performed in order to clarify the issue.

C. Contribution of thermal monopoles to pressure

Finally, let us discuss the contribution of thermal monopoles (or, dyons) to the thermodynamics of the plasma. The positive value of the excess of both electric and magnetic action densities near the monopoles means that their contributions to the trace anomaly θ , Eqs. (6), (14) and, consequently, to the pressure p and to the energy density ε , Eq. (8), are negative quantities [32]:

$$\begin{aligned}\delta\theta_{\text{mon}}(T) &< 0, \\ \delta p_{\text{mon}}(T) &< 0, \\ \delta\varepsilon_{\text{mon}}(T) &< 0,\end{aligned}\tag{38}$$

because the β -function $\tilde{\beta}(g)$ in Eq. (6) is a negative-valued function. We cannot calculate numerical values of the monopole contribution to these thermodynamic quantities because we should also take into account the entropy of the monopoles. This task cannot be completed using our method. We can only state the qualitative features of the effect of the monopoles (38).

V. CONCLUSION

In this paper we have studied the correlation of thermal abelian monopoles detected after MAG projection with the gauge invariant nonabelian action. The study has been performed for QCD with two colors and in the quenched limit. We have found an equal excess of electric and magnetic action around thermal monopoles, suggesting that the underlying non-abelian gauge configurations – associated to thermal monopoles – may correspond to selfdual dyons. The electric-magnetic equality holds with a good numerical precision (less than 4%).

We notice that the presence of the selfdual dyons in the thermal plasma is a nontrivial fact. Indeed, one can argue [19] that the thermal medium is populated with gluonic monopoles, which become dyons via the Witten effect [33] as these monopoles pass through self-dual regions (say, instantons) in space-time. In this case the monopole would get a space-dependent electric charge which, however, will be vanishing far from the instantons. In this scenario the electric action density should be small compared to the rival magnetic component. On the contrary, we have observed exact selfduality indicating that – at least at short distances – the electric component is as strong as the magnetic one. Note that the electric-magnetic duality may be a property peculiar to thermal monopoles observed in the deconfined phase of Yang-Mills theories.

We have found that thermal monopoles (dyons) make a negative contribution to the pressure and to the energy

density of the gluon plasma.

Most importantly, certain signatures of the dyons may be observed experimentally in the heavy-ion collisions via the so-called chiral magnetic effect. Indeed, since the dyons are characterized by nonzero topological charge density, they are playing a role of “seeds” of topological charge fluctuations in the plasma. In a strong magnetic field the topological structures in the gluonic vacuum leave their footprints via certain CP -odd correlations like, for example, the generation of the electric current due to the chiral magnetic effect [21]. Preliminary signatures of such a current were already observed experimentally by the STAR collaboration at RHIC [22] (this effect was also observed in the lattice gauge theory in Ref. [23]).

In order to clarify further the nature of these objects we are planning to calculate correlations of the thermal monopoles with the local topological charge density. We are also going to measure cross-correlations of fluctuations of electric and magnetic action densities around the thermal monopoles, and extend our study of correlation functions to larger distances from the monopoles.

Acknowledgments

This work has been started during the workshop “Non-Perturbative Methods in Strongly Coupled Gauge Theories” at the Galileo Galilei Institute (GGI) in Florence and was supported by the STINT Institutional grant IG2004-2 025, by the RFBR 08-02-00661-a, DFG-RFBR 436 RUS, by a grant for scientific schools NSh-679.2008.2, by the Federal Program of the Russian Ministry of Industry, Science and Technology No. 40.052.1.1.1112 and by the Russian Federal Agency for Nuclear Power. Numerical simulations have been performed on a computer farm in Genova provided by INFN.

APPENDIX A: NUMERICAL SIMULATIONS

Our numerical simulations were performed in $SU(2)$ lattice gauge theory with the standard plaquette action. The basic setup is the same as the one adopted in Ref. [4]. We used various lattice geometries $L_s^3 \times L_t$ with varying temporal extension of the lattice $L_t = 4, \dots, 13$, and fixed spatial extension $L_s = 64$. We performed simulations at different values of the lattice gauge coupling (7), $\beta = 2.7, 2.86, 2.93, 3.00, 3.05$.

The physical value of the lattice spacing was determined from the relation

$$a(\beta)\Lambda_L = R(\beta)\lambda(\beta),\tag{A1}$$

where R is the two-loop perturbative β -function, while λ is a non-perturbative correction factor computed and reported in Ref. [34]. The mass scale Λ_L is related to the critical temperature [34], $T_c = 21.45(14)\Lambda_L$, and

to the zero-temperature string tension σ via $T_c/\sqrt{\sigma} = 0.69(2)$ [35]. The set of our values of β corresponds to five lattice spacings in the interval $a = (0.015 \dots 0.045)$ fm. The set of temporal extensions L_t and the lattice spacings a determines a grid of temperature values $T = 1/(L_t a)$ which is rather wide, $T/T_c = 1.095, \dots, 5.637$.

The currents of the Abelian monopole were identified by the standard De Grand-Toussaint construction [36] after performing an Abelian projection in the Maximal Abelian gauge. This gauge is defined by the condition of the maximization of the following functional with respect to gauge transformations:

$$F_{\text{MAG}} = \sum_{\mu, x} \text{Re tr} [U_\mu(x) \sigma_3 U_\mu^\dagger(x) \sigma_3] \quad (\text{A2})$$

The maximization is achieved by an iterative combination of local maximization and overrelaxation [37].

In the Maximal Abelian gauge the monopole currents j_μ are defined as location of sources of the magnetic fields in the diagonal components of the gauge fields [36]:

$$j_\mu = \frac{1}{2\pi} \varepsilon_{\mu\nu\rho\sigma} \hat{\partial}_\nu \bar{\theta}_{\rho\sigma}. \quad (\text{A3})$$

Here $\bar{\theta}_{\mu\nu}$ is a compactified plaquette angle, $-\pi < \bar{\theta}_{\mu\nu} \leq \pi$, defined as follows:

$$\theta_{\mu\nu} = \bar{\theta}_{\mu\nu} + 2\pi n_{\mu\nu}, \quad n_{\mu\nu} \in \mathbb{N}. \quad (\text{A4})$$

-
- [1] D. E. Kharzeev, “Hot and dense matter: from RHIC to LHC: Theoretical overview”, arXiv:0902.2749; E. Shuryak, *Prog. Part. Nucl. Phys.* **62**, 48 (2009) [arXiv:0807.3033].
- [2] M. N. Chernodub and V. I. Zakharov, *Phys. Rev. Lett.* **98**, 082002 (2007) [arXiv:hep-ph/0611228].
- [3] J. Liao and E. Shuryak, *Phys. Rev. C* **75**, 054907 (2007) [arXiv:hep-ph/0611131].
- [4] A. D’Alessandro, M. D’Elia, *Nucl. Phys. B* **799**, 241 (2008) [arXiv:0711.1266] and arXiv:0812.1867.
- [5] M. N. Chernodub, A. Nakamura and V. I. Zakharov, *Phys. Rev. D* **78**, 074021 (2008) [arXiv:0807.5012].
- [6] M. N. Chernodub, K. Ishiguro, A. Nakamura, T. Sekido, T. Suzuki and V. I. Zakharov, *PoS LAT2007*, 174 (2007) [arXiv:0710.2547].
- [7] A. Gorsky and V. I. Zakharov, *Phys. Rev. D* **77**, 045017 (2008) [arXiv:0707.1284]; A. S. Gorsky, V. I. Zakharov and A. R. Zhitnitsky, *Phys. Rev. D* **79**, 106003 (2009) [arXiv:0902.1842 [hep-ph]].
- [8] M. N. Chernodub and V. I. Zakharov, “Monopoles and vortices in Yang-Mills plasma”, arXiv:0806.2874; “Magnetic strings as part of Yang-Mills plasma”, [arXiv:hep-ph/0702245].
- [9] C. Ratti and E. Shuryak, *Phys. Rev. D* **80**, 034004 (2009) [arXiv:0811.4174 [hep-ph]]; M. N. Chernodub, H. Verschelde and V. I. Zakharov, arXiv:0905.2520 [hep-ph];
- [10] G. ’t Hooft, in *High Energy Physics*, ed. A. Zichichi, EPS International Conference, Palermo (1975); S. Mandelstam, *Phys. Rept.* **23**, 245 (1976).
- [11] A. Di Giacomo, B. Lucini, L. Montesi and G. Paffuti, *Phys. Rev. D* **61**, 034503 (2000) [arXiv:hep-lat/9906024]; *Phys. Rev. D* **61**, 034504 (2000) [arXiv:hep-lat/9906025].
- [12] M. D’Elia, A. Di Giacomo, B. Lucini, G. Paffuti and C. Pica, *Phys. Rev. D* **71**, 114502 (2005) [arXiv:hep-lat/0503035].
- [13] M. N. Chernodub, M. I. Polikarpov and A. I. Veselov, *Phys. Lett. B* **399**, 267 (1997) [arXiv:hep-lat/9610007].
- [14] P. Cea and L. Cosmai, *JHEP* **0111**, 064 (2001); P. Cea, L. Cosmai and M. D’Elia, *JHEP* **0402**, 018 (2004) [arXiv:hep-lat/0401020].
- [15] J. Greensite, *Prog. Part. Nucl. Phys.* **51**, 1 (2003) [arXiv:hep-lat/0301023].
- [16] V. G. Bornyakov, V. K. Mitrjushkin, M. Muller-Preussker, *Phys. Lett. B* **284**, 99 (1992); S. Ejiri, *Phys. Lett. B* **376**, 163 (1996) [arXiv:hep-lat/9510027].
- [17] To be more precise, in this paper we use the word “dyon” in order to describe an object in the Euclidean spacetime, which is characterized by the same (on the quantitative level) $1/r^{-4}$ behavior of the electric and magnetic non-abelian action densities.
- [18] A. Gonzalez-Arroyo and Yu. A. Simonov, *Nucl. Phys. B* **460**, 429 (1996) [arXiv:hep-th/9506032].
- [19] V. Bornyakov and G. Schierholz, *Phys. Lett. B* **384**, 190 (1996) [arXiv:hep-lat/9605019]; M. N. Chernodub, F. V. Gubarev and M. I. Polikarpov, *JETP Lett.* **69**, 169 (1999) [arXiv:hep-lat/9801010].
- [20] V. G. Bornyakov, E. M. Ilgenfritz, B. V. Martemyanov and M. Muller-Preussker, *Phys. Rev. D* **79**, 034506 (2009) [arXiv:0809.2142 [hep-lat]]; V. G. Bornyakov, E. M. Ilgenfritz, B. V. Martemyanov, S. M. Morozov, M. Muller-Preussker and A. I. Veselov, *Phys. Rev. D* **76**, 054505 (2007) [arXiv:0706.4206 [hep-lat]]; E. M. Ilgenfritz, B. V. Martemyanov, M. Muller-Preussker and A. I. Veselov, *Phys. Atom. Nucl.* **68**, 870 (2005).
- [21] D.E. Kharzeev, L.D. McLerran, and H.J. Warringa, *Nucl. Phys. A* **803**, 227 (2008) [arXiv:0711.0950]; K. Fukushima, D.E. Kharzeev, and H.J. Warringa, *Phys. Rev. D* **78**, 074033 (2008) [arXiv:0808.3382].
- [22] S. A. Voloshin [STAR Collaboration], arXiv:0806.0029 [nucl-ex]; H. Caines [STAR Collaboration], arXiv:0906.0305 [nucl-ex].
- [23] P. V. Buividovich, M. N. Chernodub, E. V. Luschevskaya and M. I. Polikarpov, *Phys. Rev. D* **80**, 054503 (2009) [arXiv:0907.0494]; *Pis’ma v ZhETF* **90**, 456 (2009).
- [24] H. U. Yee, “Holographic Chiral Magnetic Conductivity,” arXiv:0908.4189 [hep-th]; A. Rebhan, A. Schmitt and S. A. Stricker, arXiv:0909.4782 [hep-th].
- [25] G. Boyd, J. Engels, F. Karsch, E. Laermann, C. Legeland, M. Lutgemeier and B. Petersson, *Nucl. Phys. B* **469**, 419 (1996) [arXiv:hep-lat/9602007].
- [26] V. G. Bornyakov, V. K. Mitrjushkin and M. Muller-Preussker, *Phys. Lett. B* **284**, 99 (1992).
- [27] S. Ejiri, *Phys. Lett. B* **376**, 163 (1996) [arXiv:hep-lat/9510027].
- [28] B. L. G. Bakker, M. N. Chernodub and M. I. Polikarpov, *Phys. Rev. Lett.* **80**, 30 (1998) [arXiv:hep-lat/9706007].
- [29] B. L. G. Bakker, M. N. Chernodub, M. I. Polikarpov, A. I. Veselov, *Phys. Lett. B* **449**, 267 (1999)

- [arXiv:hep-lat/9811001].
- [30] V. G. Bornyakov, M. N. Chernodub, F. V. Gubarev, M. I. Polikarpov, T. Suzuki, A. I. Veselov and V. I. Zakharov, Phys. Lett. B **537**, 291 (2002) [arXiv:hep-lat/0103032].
- [31] E. B. Bogomolny, Sov. J. Nucl. Phys. **24**, 449 (1976); M. K. Prasad and C. M. Sommerfield, Phys. Rev. Lett. **35**, 760 (1975); P. Rossi, Phys. Rept. **86**, 317 (1982).
- [32] The positive value of the monopole contribution reported in Ref. [6] can be explained by the fact that in that study the contribution of the ultraviolet monopoles was not subtracted.
- [33] E. Witten, Phys. Lett. B **86**, 283 (1979).
- [34] J. Engels, F. Karsch and K. Redlich, Nucl. Phys. B **435**, 295 (1995) [arXiv:hep-lat/9408009].
- [35] J. Fingberg, U. M. Heller and F. Karsch, Nucl. Phys. B **392**, 493 (1993) [arXiv:hep-lat/9208012].
- [36] T. A. DeGrand and D. Toussaint, Phys. Rev. D **22**, 2478 (1980).
- [37] P. Cea and L. Cosmai, Phys. Rev. D **52**, 5152 (1995) [arXiv:hep-lat/9504008].